VISCOUS AND INVISCID LINEAR/NONLINEAR CALCULATIONS VERSUS QUASI 3D EXPERIMENTAL CASCADE DATA FOR A NEW AEROELASTIC TURBINE STANDARD CONFIGURATION

T.H. Fransson, M. Jöcker
Chair of Heat and Power Technology
Royal Institute of Technology
Stockholm, Sweden

A. Bölcs, P. Ott
Laboratoire de Thermique Appliquée et de Turbomachines
Swiss Federal Institute of Technology
Lausanne, Switzerland

ABSTRACT

This paper presents a new International Standard Configuration to be added to an already existing set of 10 configurations for unsteady flow through vibrating axial-flow turbomachine cascades. This 11th configuration represents a turbine blade geometry with transonic design flow conditions with a normal shock positioned at 75% real chord on the suction side. Out of a set of test cases covering all relevant flow regimes two cases were selected for publication: A subsonic, attached flow case and an off-design transonic case showing a separation bubble at 30% real chord on the suction side are published. The performed tests are shown to be repeatable and suitable for code validations of numerical models predicting flutter in viscous flows.

The validity of the measured data of the two public cases was examined and comparisons with other tests were conducted. Sometimes a large difference in aerodynamic damping was observed on cases with similar flow conditions. This was investigated at three transonic cases with almost identical inlet flow conditions and only small variations in outlet Mach Number. It was found that the differences in the global damping are due to very local changes on the blade surface in the shock region, which obtain a large influence by the integration because of the discrete measuring points. Hence it is recommended not to look at the global damping for code validations but more precisely to the local values. These show a common tendency, which is reproducible with different numerical methods.

This was demonstrated with a potential model, a linear Euler model, a nonlinear Euler model and a Navier-Stokes solver, all applied to predict flutter of each test case with a 2D/Q3D approach. The limitations of inviscid codes to predict flutter in viscous flow regimes is demonstrated, but also their cost advantage in attached flow calculations. The need of viscous code development and validation is pointed out. This should justify and encourage the publication of thoroughly measured test cases with viscous effects.

NOMENCLATURE

A_i		area elements of data points i projected into bending direction, normalized with c (sign: on ss >0, on ps < 0)	-
c		chord	m
cp	$\frac{(p - p1)}{(pt1 - p1)}$	steady pressure coefficient	-
$\tilde{c}_p(x,t)$	$\frac{c \cdot \tilde{p}(x,t)}{h \cdot (pt1 - p1)}$	unsteady pressure coefficient	-
$\tilde{c}_p, \tilde{c}_{pi}$		amplitude of unsteady pressure coefficient (1st harmonic)	-
e		probe distance	m
f		frequency	Hz
h		bending amplitude	m
H		enthalpy	J/kg/K
IBPA, σ		interblade phase angle	deg.
k	$\frac{2 \cdot \pi \cdot f \cdot c}{2 \cdot v_{2\,exp}}$	reduced frequency based on half chord and experimental outlet velocity	-
M		Mach number	-
p		pressure	Pa
sf	$\frac{(pt1 - p1)_{NOVAK}}{(pt1 - p1)_{EXP}}$	scaling factor in NOVAK	-
v		velocity	m/s
x		chordwise coordinate	m
XI, Ξ_h	$-\sum_i \tilde{c}_{pi} \cdot A_i \cdot \sin\phi_i$	aerodynamic damping due to bending >0: stable, <0: unstable	-
ß		relative flow angle	deg.
γ		stagger angle	deg.
δ		bending direction	deg.
ϕ, ϕ_i, phi~		phase of unsteady pressure coefficient (1st harmonic)	deg.
τ		pitch	m
Indices			
1		inlet	
2		outlet	
i		data point	
is		isentropic	
t		total values	
tan		tangential	
~		unsteady perturbation value (without steady part)	

INTRODUCTION

Several unsteady prediction models for flutter at attached flow conditions have appeared in the open literature (and as confidential design methods in the industry) over the last decade (see for example Verdon and Caspar, 1984; Whitehead and Newton 1985; Fransson and Pandolfi, 1986; Smith, 1989; Hall et al., 1989; He, 1989; Whitehead, 1990; Sidén, 1991; Holmes et al., 1991; Huff et al., 1991; Carstens at al., 1993; Giles et al., 1993; Kahl et al., 1993; Gerolymos et al., 1994; Groth et al., 1996; Grüber et al., 1996). Several of these models show good to excellent agreement against selected test cases of mainly two-dimensional nature. However, the number of internationally accepted test cases for turbomachine blade flutter studies is largely limited to a data base established as part of the Symposium series "Unsteady Aerodynamics and Aeroelasticity in Turbomachine Cascades". This database is documented in two reports by Bölcs and Fransson [1986] and Fransson and Verdon [1991]. A large need for more well documented experimental data for code validation and for a better physical understanding of unsteady flow phenomena, and especially the propagation of disturbances, through vibrating cascades exists throughout the aeroelastic research community.

Some years ago extensive experiments on a two-dimensional section of a vibrating last-stage gas turbine blade (54% span) were performed in the annular test rig at the EPF-Lausanne [Bölcs et al, 1991, 1993]. Many experiments have also been performed on the same geometry in the linear test facility at the EPFL [Norryd, 1997; Ott et al, 1998]. This substantial database, especially the one from the annular test facility, has been used by a few researchers for code validation over the years [Bölcs et al., 1991; Carstens et al., 1993; Leyland et al., 1994; Grüber et al., 1996]. However, the blade geometry has not been available to the larger research community till presently.

OBJECTIVE

The objective of the present paper is to, for the first time, make general unsteady data of the well documented experiments, performed in an annular test facility, on a low pressure gas turbine blade section available to the larger research community. In this process, the experimental results should be scrutinized in detail against some selected numerical models of different complexities, with the aim to establish inconsistencies between the experiments and the models, as well as eventual differences between the various models.

METHOD OF ATTACK

Out of the large quantity of experimental results available a few test cases have been selected with the aim to illustrate the quality of the data, both as regards to the repeatability of the steady-state and unsteady results, and regards changes in unsteady behavior due to small variations in the outlet flow conditions. Such a process is of importance for any experimental results presented with the aim of comparison with theory or numerical results, and specifically for unsteady experiments, where data can only be obtained at discrete locations on a blade surface. Results from three series of subsonic, transonic and supersonic outlet Mach numbers will be analyzed, with emphasis on the most critical conditions (transonic). Along these lines the importance of looking at the detailed unsteady pressure distribution along the blade surface is illustrated by demonstrating that the global aerodynamic damping determined from discrete pressure transducer locations in the experiments can vary significantly because of small inevitable inconsistencies in the experimental conditions.

Thereafter numerical results from 4 different numerical methods are presented and compared to the experimental data.

Finally, two selected experiments are proposed as test cases for the new 11th Standard Configuration on Unsteady Flow Through Vibrating Turbomachine Cascades. They represent one subsonic case for code calibration and one transonic off design case with high incidence inlet flow angle and a separation bubble on the suction surface leading edge, which should be a challenge for viscous prediction models development. These cases including full geometry will be provided on the Internet together with the International Standard Configurations 1-10. (Internet address: http://www.egi.kth.se/ekv/stcf).

BRIEF DESCRIPTION OF TEST FACILITY AND GEOMETRY

Several flow cases were studied in the annular non rotating cascade facility at EPF-Lausanne, which is schematically drawn in figure 1. The main features can be summarized as follows: Inlet and outlet conditions can be varied over a large range, where a two settling chamber system allows to adjust the radial flow distribution at the inlet to the blade channel. The outer diameter of the test section is 400 mm, the blade span is 40 mm.

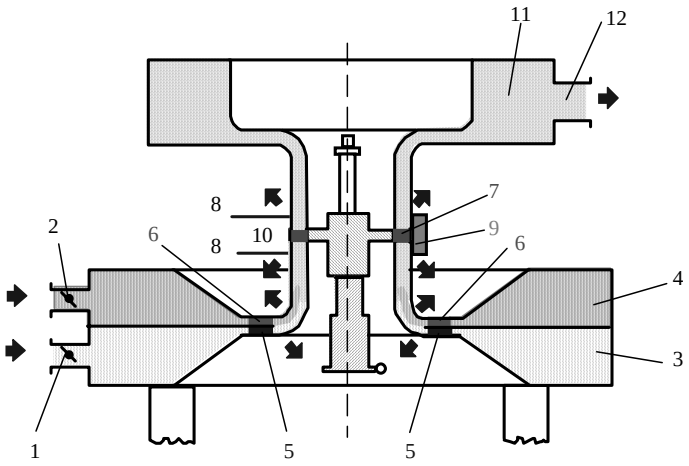

1.2 Inlet valves
3.4 Settling cambers
5,6 Inlet guide vanes
7 Test cascade
8 Aerodynamic probes
9 Cylindrical optic
10 Wall pressure taps
11 Outlet flow collector
12 Outlet vanes
→ Boundary layer suction

Fig. 1: Schematic view of the test facility at LTT/EPFL [Bölcs et al, 1986]

The test facility is supplied with air by a four stage radial compressor with a maximum mass flow rate of 10 kg/s and a maximum pressure ratio of 3.5. An additional compressor is used to suck off the wall boundary layers (fig. 1).

In order to simulate unsteady flow conditions in the test cascade, all 20 blades are electromagnetically excited and controlled to vibrate in traveling wave mode. This includes the control of vibration amplitude, vibration frequency and the interblade phase angle. The

suspensions of the blades are designed to reproduce the eigenfrequency and bending direction of the first bending mode of the blade performing a solid blade motion. Also single blade vibration data were collected to obtain the influence coefficients. More detailed information of the test facility can be found in Bölcs et al. [1983, 1986, 1991, 1993].

Geometry and measuring planes of the presented configuration are illustrated in figure 2. Geometry data has recently been made available for all interested researchers and will be published on Internet aligned with this document.

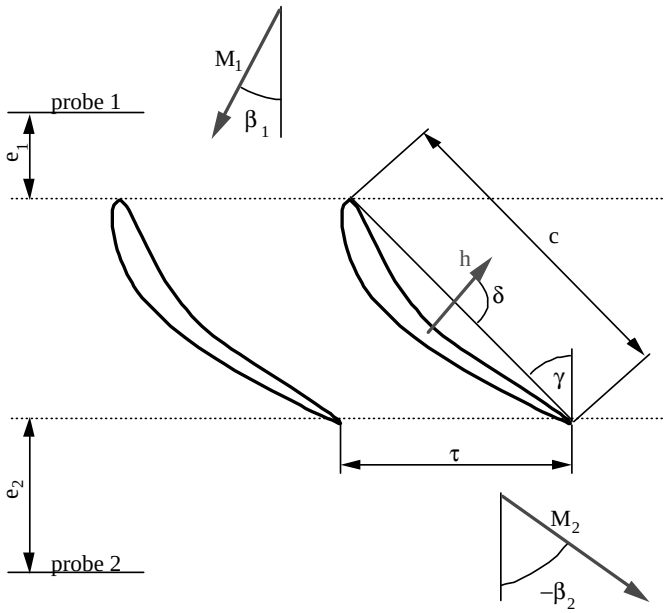

Fig. 2: STCF 11 turbine geometry at midspan [Körbächer et al, 1993]

Measurements of static and total pressures as well as the flow angles were done in the planes e1 and e2 before and behind the cascade (fig. 2). The blade surface distributions of steady and unsteady pressures were measured with pressure taps for the steady state and miniaturized piezo-resistive pressure transducers for the time dependent data measurements, all embedded at midspan on different blades. The measured flow cases on this configuration vary in incidence flow angles from 6 deg. to 48 deg. and in isentropic outlet Mach Number from 0.64 to 1.46. The blade was designed for nominal flow conditions with an incidence angle of 16.8 deg. and M_{2is}=1.0.

QUALITY OF EXPERIMENTAL RESULTS

Steady Results

A review of the available steady test data shows that the obtained results are highly repeatable [Bölcs et al, 1991]. Figure 3 gives an example of steady, transonic off design data, which also demonstrates this on very sensible flow cases. Due to small changes of the flow conditions the position of the shock impingement was determined to vary with about 5% chord length for these cases. The number of measuring points on the blade surfaces is sufficient to detect the shock and the separation which occur on the suction side surface. The shown off-design cases indicate a separation bubble to be present from leading edge to 30% of true chord and a shock at about 75 % of true chord. A more detailed discussion on these results and their repetivity can be found in [Bölcs et al., 1991; 1993]. The underlined case in figure 3 is made public with this document.

Reasons for the deviations between experimental data and numerical results even for subsonic attached flow (see page 7) are not known in detail. They might be found in real flow effects which can not be captured by the applied numerical models or are lost due to the measuring technique (f. ex. 3D effects, side wall boundary layers, inaccuracies in measurement of pressures, estimation of flow angles, averaging of flow values over pitch and span).

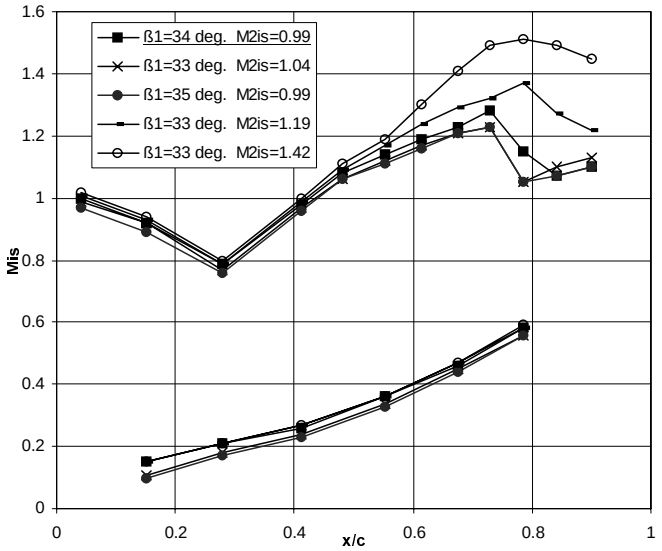

Fig. 3: Transonic off-design test cases on STCF 11

Unsteady Results

Also the unsteady results presented here are shown to be highly repeatable [Bölcs et al, 1991]. But for similar flow cases partly large differences of aerodynamic damping were observed.

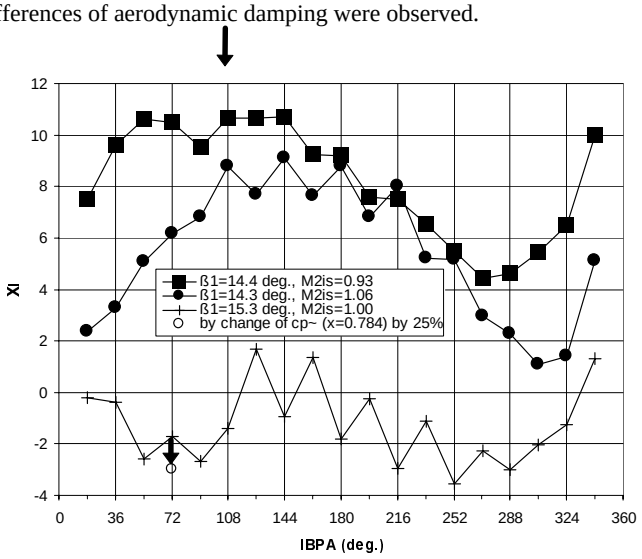

Fig. 4: Global damping of transonic cases

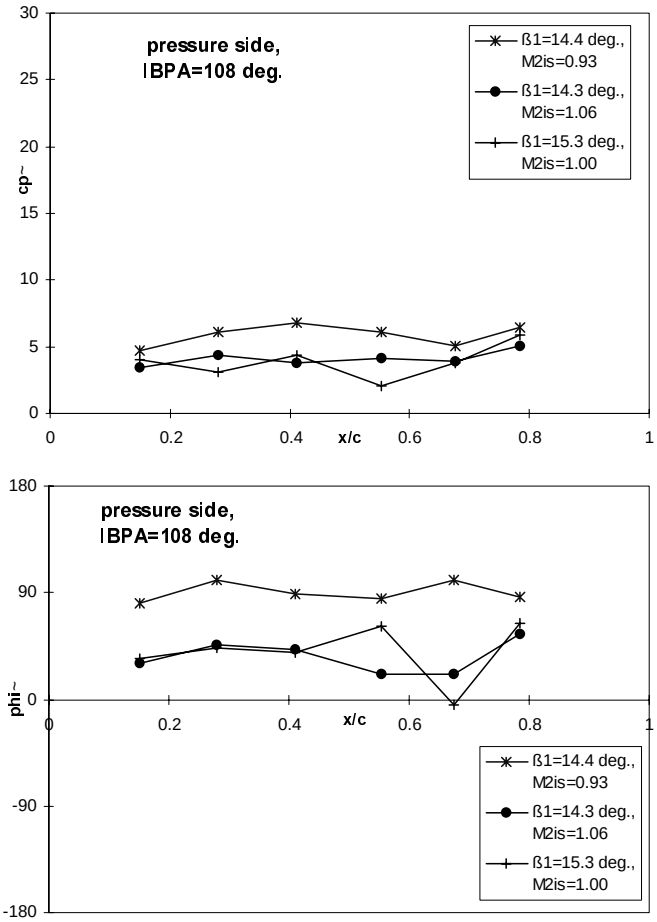

Fig 5: Unsteady pressure (amplitude and phase of 1st harmonic) pressure side

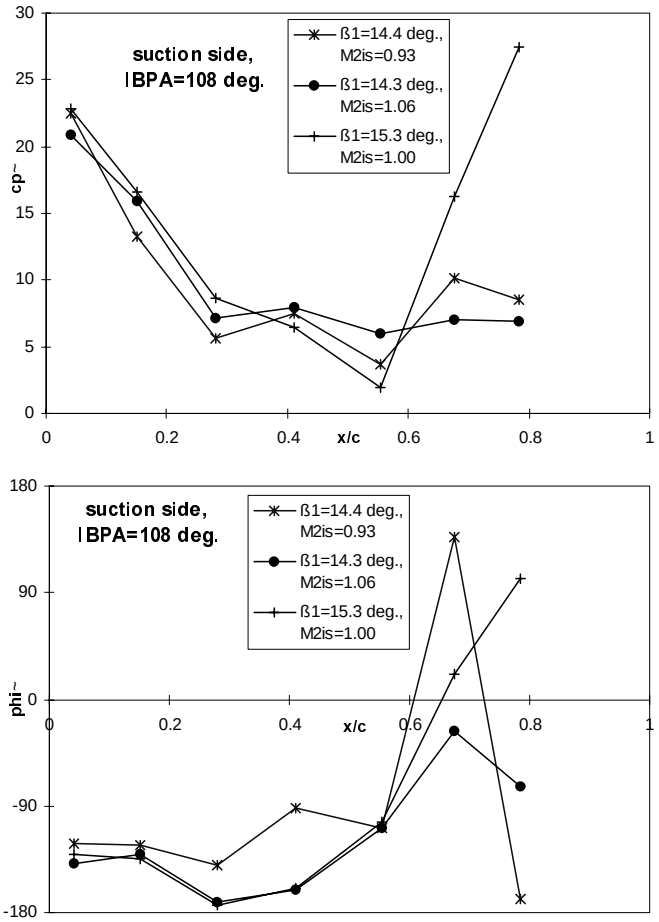

Fig 6: Unsteady pressure (amplitude and phase of 1st harmonic) suction side

These were strongest in the transonic flow regimes compared to subsonic or supersonic flow cases. Figure 4 plots the aerodynamic damping for three cases in the transonic flow region with similar inlet flow conditions. From such a figure it would be tempting to draw the conclusion that the experimental data are useless. However, to analyze the differences more in detail the local values of pressure coefficients have been compared. Figures 5 and 6 show these for an interblade phase angle of 108 deg., where the differences in global aerodynamic damping were found to be large (compare figure 4).

It can be observed that all three cases show the same tendency in amplitude as well as in phase of the unsteady pressure response: The pressure side response shows a relatively small and constant amplitude with stabilizing phase. All cases show high but stabilizing amplitudes close to the leading edge on the suction side, whereas the response is tendentiously destabilizing in the shock region on the suction side with relatively high amplitudes.

It is obvious that the main differences in aerodynamic damping are caused by differences in the data from the shock region, which has the highest influence on the damping ($\propto \tilde{c}_{pi} \cdot \sin\phi_i$). These data are highly dependent on the exact position of the shock relative to the pressure transducers location. As discussed in the steady state experimental results the shock impingement position itself is very sensible, especially for high incidence flow cases [Bölcs et al., 1991].

Hence due to the limited number of pressure transducers on the pressure side (max. 6 transducers/channel) and on suction side (max. 7 transducers/channel) the integration of the experimental data over the blade surface does not always lead to accurate results. Moreover the obtained value is very sensible to small changes in the flow and the following changes in shock position.

The following example case study on the 3rd case in figure 4 (M_{2is}=1.00) demonstrates this: To change the aerodynamic damping at an IBPA of 72 deg. from the original value of -1.687 to -3 (see arrow in fig. 4), which would fit the value into a harmonic pattern, the following local change close to the shock (point x/c=0.78) would be sufficient: increase of $\tilde{c}_p$ by about 25% (from 20.55 to 25.55). This corresponds only to a small shift in shock position, what can be judged from figure 6. This cannot be generalized because the single point influence depends strongly on the level of the other measurement values as well as on the phase, but it gives an impression of the data sensibility.

Hence the sensibility of the aerodynamic damping explains also the zic-zac pattern seen, when looking at the damping versus IBPA

(fig. 4): the experimental data was taken in two series, first in steps of 36 deg. (36, 72, ... deg. of IBPA), then the cases in between (18, 54,... deg. of IBPA) with a time delay of 20 minutes between neighboring IBPAs. It is reasonable to conclude that these two series had slightly different shock positions. This is confirmed by the fact that this pattern is only recognized in transonic flow cases with one subsonic exception.

From the authors previous and present experience and from the above reasoning it is strongly suggested to compare only local values for the validation of numerical methods and evaluate integrated results only from validated codes. The local values shown here underline the quality of the data representing a good consistency even at sensible flow conditions. It also should be noticed that for all measured unsteady data accuracy is given in terms of a 95% confidence interval, obtained from a statistical evaluation. This information is however not presented in the diagrams.

NUMERICAL MODELS

Different numerical models were applied in order to compare the experimental results with theoretical data. These cover nearly the whole range of 2D/Q3D aerodynamic flutter models actually used in turbomachinery research. Table 1 puts together the characteristic information of the presented calculations. The aim of the calculations was to verify the quality of the experiments and to demonstrate the applicability of the numerical methods. The influence of the used unsteady boundary conditions (reflective or non reflective) is assumed to be small due to an investigation by [Krainer, 1998]. A physical reason for this is the substantial contribution of the quasi steady loading to the unsteady loading in high turning turbine cascades.

			FINSUP	NOVAK	INST	VOLFAP
		exp. data	potential code	lin Euler	nonlin. Euler	viscous code
boundary conditions	stdy.	-	$v_{tan,1}$,	α_1, p_2	α_1, p_{t1}, p_2	α_1, p_{t1}, H_{t1}, p_2
	unst.*	-	1*	2*	3*	2*
Number of mesh nodes		-	629	2324	2500	2275 o +6075 i
timesteps	stdy.		-	-	10000	8000
	unst.		-	-	1.5E06	60000
CPU time on IBM RS 6000 / 230	stdy.		5 s	9 min	16 h	8 ¾ h
	Unst. /IBPA		9 s	40min	292 h (guess)	65 h (guess)
Subsonic case	M1	0.31	0.31	0.291	0.29	0.29
	ß1	15.2	15.2	15.2	15.2	15.2
	M2is	0.69	0.69	0.689	0.671	0.69
	k	0.2134	0.2134	0.2134	0.2134	0.2134
	h/c	0.0054	1	0.005	0.0054	0.0054
Off-Design case	M1	0.4	0.4	0.387	0.378	0.37
	ß1	34	33	33	34	33
	M2is	0.99	0.99	0.99	0.993	0.99
	k	0.1545	0.155	0.1545	0.1545	0.1545
	h/c	0.0035	1	0.005	0.0035	0.0035
Q3D option			used	not shown	-	not shown

*1 = nonreflecting, 2=1D non reflecting, 3=2D approx. non reflecting
guess = calculated from CPU time scaling factors

Table 1 Calculations overview for the two selected steady state test cases

Q3D Potential Small Perturbation Model (FINSUP)

FINSUP calculates steady and unsteady flows in cascades using a finite element method with triangular element meshes. [Whitehead and Newton, 1985; Rolls Royce, 1989; Whitehead, 1990]. The program solves the potential equations for isentropic, irrotational 2D-flows, where a variation of streamtube thickness is possible (Q3D). For the solutions the Newton-Raphson technique is used. For the unsteady calculations blade vibrations of small amplitudes are assumed and modeled in a single blade passage (traveling wave mode), where the blades are treated as rigid bodies. Unsteady results are obtained by a time-linearized approach. Figure 7 shows the used mesh, which resulted from a mesh influence study [Jöcker, 1994]. A mesh independence of the results was not reached but the quality of results was judged to be sufficient with respect to the method.

In FINSUP the Q3D option was used in order to obtain the correct inlet and outlet flow conditions. This did not lead to an improvement of the steady or unsteady predictions but to a decrease in static pressure on the suction surface close to leading edge [Jöcker, 1994]. However, this led to the right estimation of the dynamic inlet pressure (p_{t1}-p_1), which is used to normalize the blade surface pressure to obtain the pressure coefficient. Another method applied in order to normalize pressures with identical factors was to introduce a scaling factor. This was done for the results obtained with the linear Euler code (NOVAK), which is described below.

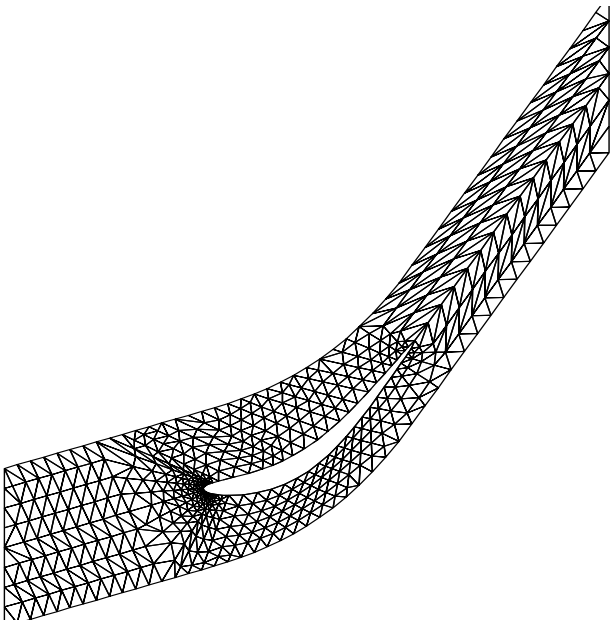

Fig. 7: Potential flow model unstructured mesh, 629 nodes

Linearized Euler Model (NOVAK 2D60)

NOVAK 2D60 is a time-linear solver for the 2D/Q3D Euler Equations, where small periodic perturbations are assumed to disturb the mean steady flow. The blade motion is modeled in the traveling wave mode for both rigid or real mode vibrations. Unsteady results are obtained as the first harmonic pressure response on the blade surface in the frequency domain. The code needs a 2D unstructured grid, where mesh adaption can be applied and the multigrid option can be chosen. The presented results are obtained on meshes optimized during a mesh study [Imfeld, 1997]. Sufficient mesh independence was reached with the mesh presented in this paper. Also the influence

on unsteady results were studied and a sufficient mesh independence was found. This was however only proved for the subsonic case. Figure 8 shows this mesh. A scaling factor *sf* to account for the different dynamic inlet pressures was introduced in the post processing in order to obtain comparable pressure coefficients. The Q3D method described for FINSUP was also tested to fit the dynamic inlet pressure but is not presented here.

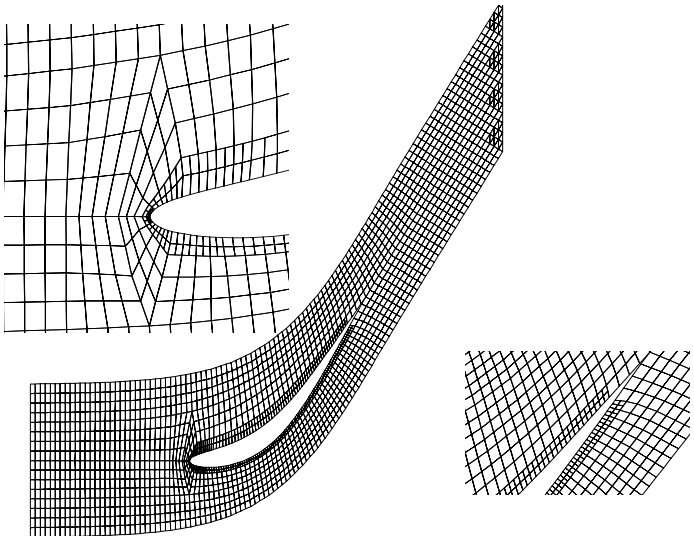

Fig. 8: Linearized Euler model structured mesh, 2324 nodes

2D Nonlinear Euler Model (INST)

INST is an explicit solver for the steady and unsteady inviscid flow around vibrating blades in a 2D cascade. It was extended to cascade flows on the basis of a nozzle flow solver [Bölcs et al., 1989].

It uses the MacCormack explicit second order time marching scheme and the flux vector splitting method of van Leer [Anderson et al., 1987] for the space derivations. At the inlet, the flow angle is held constant, at the outlet boundary, the static pressure relative to the inlet total pressure is imposed. The main features for flutter calculations are a moving H-mesh, periodic boundary conditions and the unsteady 2D approximate non reflecting boundary conditions presented by [Giles, 1989]. Blade motion is modeled in the traveling wave mode. All blades can be vibrated either in bending or torsional motion with fixed interblade phase angles.

For the presented results an H-type mesh with lines locally normal to the blade surface was applied, which is shown in figure 9. The resolution of this mesh was judged to be sufficient for the aim of the current presentation for the subsonic case. It is believed that a local refinement of the mesh would lead to an improvement of the shock capturing (see steady results). This is planned for future work.

Q3D Non Linear Viscous Flow Model

VOLFAP is a fully unsteady, quasi-3D viscous flow code solving the Navier Stokes equations for a compressible fluid [Sidén, 1991]. Turbulence is accounted for by a two-layer eddy viscosity model [Baldwin and Lomax, 1978]. 1D non reflecting boundary conditions are available in the code.

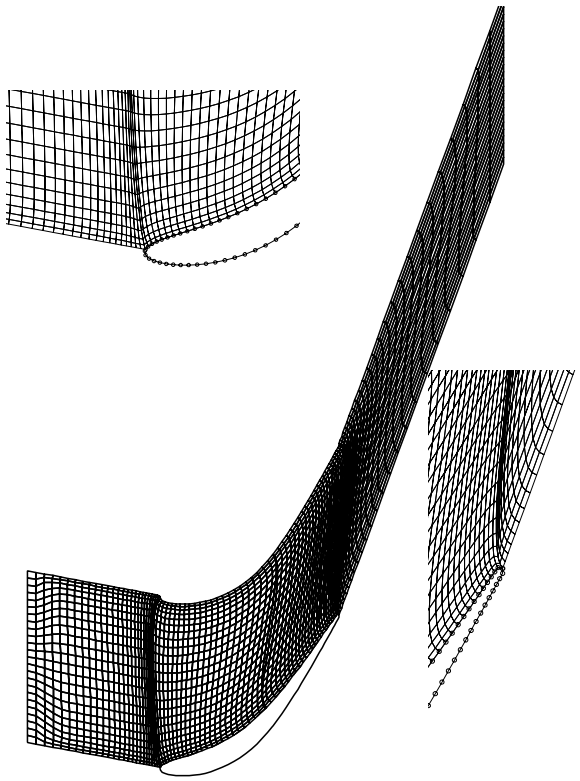

Fig. 9: Nonlinear Euler model structured mesh, 2500 nodes

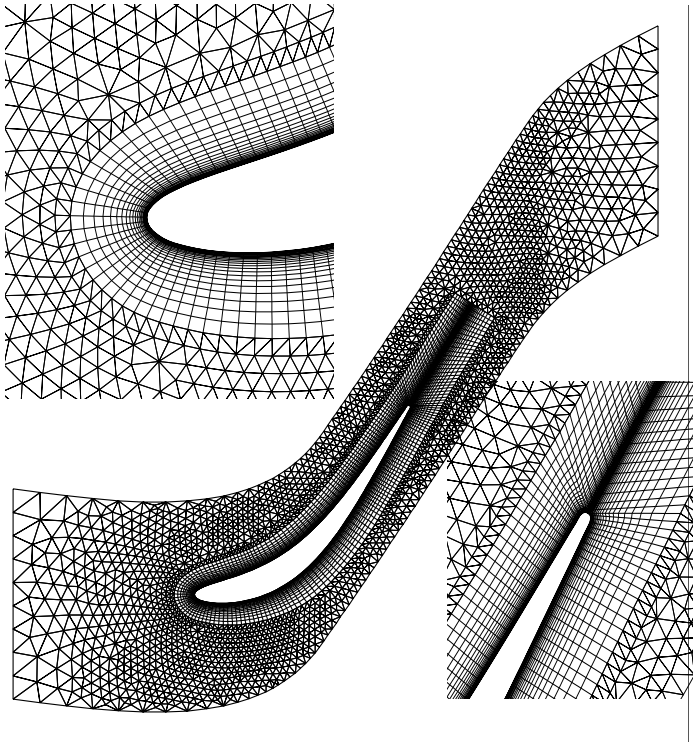

Fig. 10: Viscous mesh, inner structured mesh: 27 x 225 =6075 nodes, outer unstructured mesh: 2275 nodes

The computational mesh consists of an inner, boundary fitted mesh (structured C-mesh) and an outer mesh of triangular elements. In the inner mesh an implicit scheme by Beam and Warming [1977] is used. The outer region is calculated with an explicit scheme using the Taylor-Galerkin Finite Element Technique. Figure 10 shows the applied mesh as well as a close up of the leading edge and trailing edge mesh regions. A mesh study was conducted in [Jöcker, 1994].

COMPARISON OF NUMERICAL MODELS AND TEST CASES

Steady Results

Figure 11 shows the comparison of predicted steady results for the subsonic case in terms of isentropic Mach number distribution. It demonstrates a smooth change of flow over the blade surfaces without remarkable disturbances. All calculations show the same behavior to slightly overpredict the Mach numbers in the middle of the blade on suction side compared to the experiments. This can be due to real flow effects which can not be described by the used prediction models. Surprisingly, the linear Euler method comes closest to the experiments.

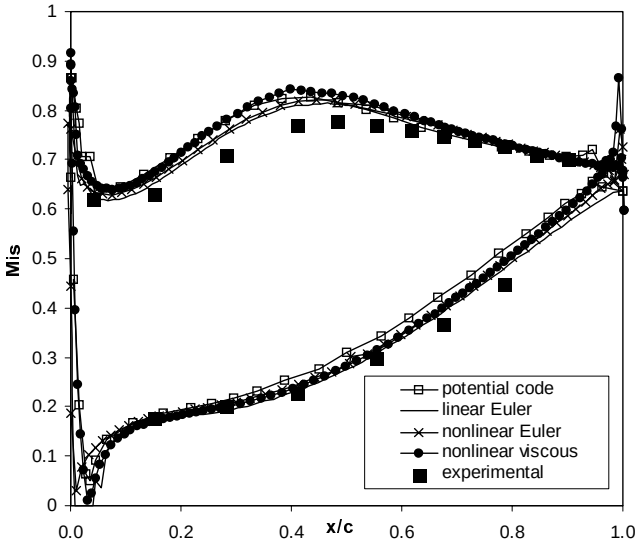

Fig. 11: Surface distribution of is. Mach number, theory vs. experiments, subsonic case

Also the off-design calculations show sufficient agreement with the experimental data with exception of the shock prediction. The potential code does not predict a shock but rather a smooth re-compression. The linear Euler code and the viscous code position the shock too far downstream, but with a better agreement of the viscous results. This was also found by Carstens [1993] and Grüber [1996]. The nonlinear Euler code predicts the shock upstream of the measured position. It is assumed that with a more elaborated mesh this shock position might be predicted better. This is planned for future work.

Only the linear Euler code represents the strength of the measured shock. None of the codes can predict the measured pre-shock Mach number. This has to be seen in the context of the shock sensibility discussed in the presentation of the experimental data: fairly small inlet flow changes gave significantly different pre shock conditions in the experiments. Parameter studies, which are planned for future work on the numerical inlet flow conditions could demonstrate their influence on the predictions.

Only the viscous code can predict the separation bubble indicated by the deceleration, which occurs on ca. 15%-30% relative chord on suction side. This will also lead to major differences in the unsteady results, as discussed below.

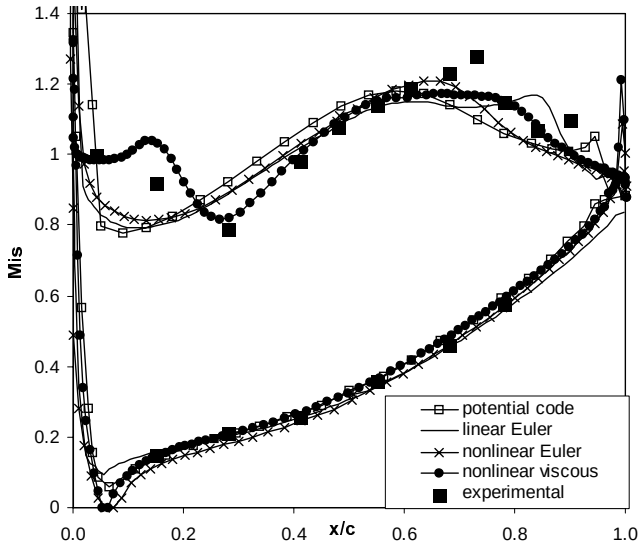

Fig. 12: Surface distribution of is. Mach number, theory vs. experiments, off-design case

Unsteady Results

For the unsteady calculations rigid body blade vibrations in traveling wave mode were assumed. Pure bending perpendicular to chord was specified. The presented results are obtained from a Fourier transformation of the time domain solution. Only the first harmonics of the pressure responses are compared in terms of amplitude and phase. In the nonlinear results higher harmonics had nearly no influence.

Figures 13 and 14 show the pressure response for the subsonic case and figures 15 and 16 for the transonic off-design case. For both cases all codes predict the for this cascade typical stabilizing pressure response on the pressure side blade surface. Differences in the predictions are mainly in the phase. The viscous code tendentiously gives a smaller phase angle than the other models.

Subsonic case: The amplitudes on suction side are represented tendentiously right with all codes, even though larger differences between the codes can be seen. In the phase prediction on suction side the inviscid results are similar, especially from the linear methods, whereas the change from stable to unstable on the blade surface is predicted further upstream with the viscous method. However, most of the experimental data show instability whereas the numerical results are more represented in the stable region. Obviously this has an influence on the aerodynamic damping.

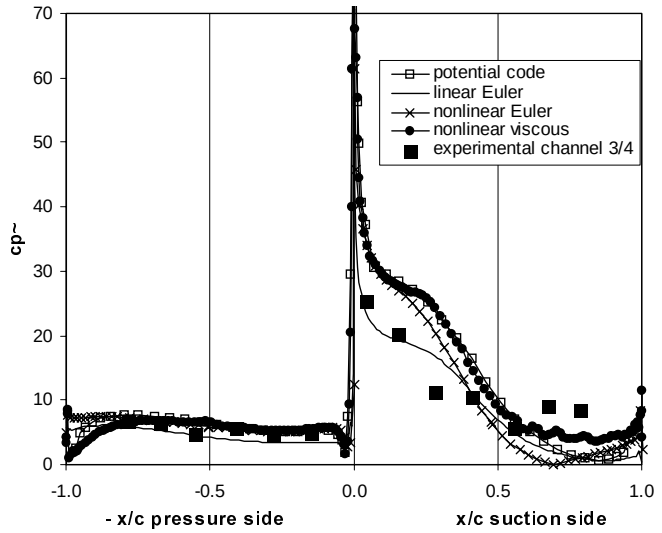

Fig. 13: Amplitude of pressure coefficient, 1st harmonic, subsonic case, IBPA=180 deg.

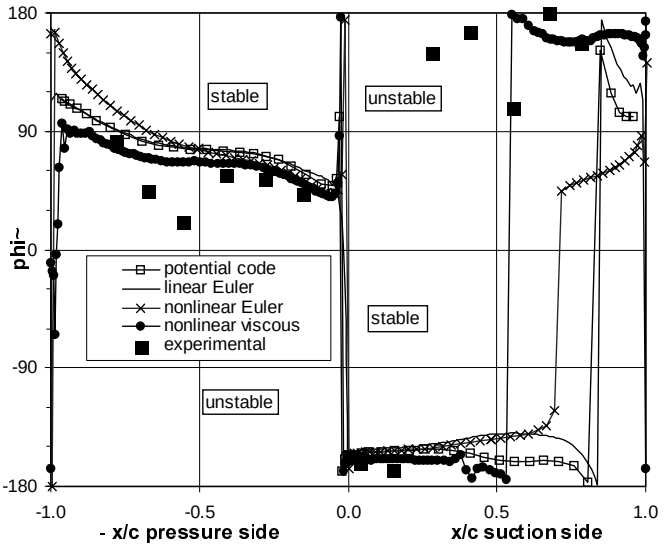

Fig. 14: Phase of pressure coefficient, 1st Harmonic, subsonic case, IBPA=180 deg.

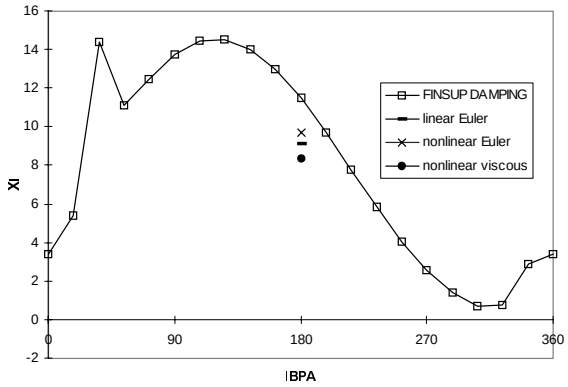

Fig. 17: Predicted aerodynamic damping, subsonic case

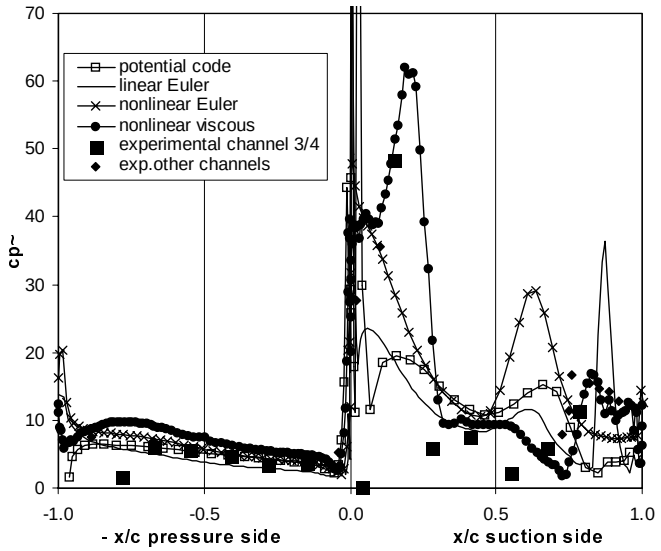

Fig. 15: Amplitude of pressure coefficient, 1st harmonic, off-design case, IBPA=180 deg.

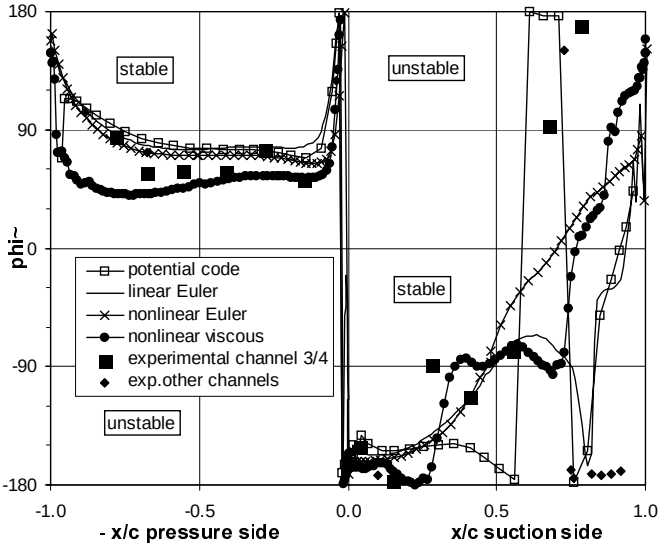

Fig. 16: Phase of pressure coefficient, 1st harmonic, off-design case, IBPA=180 deg.

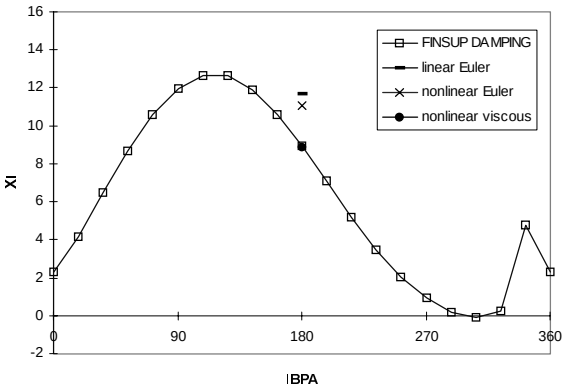

Fig. 18: Predicted aerodynamic damping, transonic case

Transonic case: All codes predict a perturbation pressure due to the impinging shock on suction side, but on different positions and different strength. The linear Euler code and the viscous code prediction compare well to the experimental shock peak, both the other codes place it too far upstream. Also here it is assumed that a better shock capturing with an improved mesh for the nonlinear Euler calculations could give a better prediction. Still it is surprising that the peak position does not coincide with steady shock position. The suction side calculations of the transonic case point out the necessity to use a viscous solver here, because only this code can take into account the separation bubble. Obviously its movement leads to a relatively high perturbation pressure at leading edge, with slightly stabilizing effect for an IBPA of 180 deg.

Table 2 lists the estimated aerodynamic damping XI obtained with the different numerical methods. All damping values were integrated with the same integration scheme. The differences are as high as up to 28 %. Figures 17 and 18 show these values in comparison to the prediction by the potential code for all interblade phase angles. Again it can be seen that the aerodynamic damping does not point out the detailed differences in the predictions.

	PREDICTED AERODYNAMIC DAMPING XI				
Case	IBPA	FINSUP	NOVAK	INST	VOLFAP
subsonic	180 deg.	10.8	9.1	9.7	8.4
transonic	180 deg.	8.4	11.7	11.0	8.9

Table 2: **Predicted aerodynamic damping XI**

CONCLUSIONS

A new International Standard Configuration is presented to be added to the already existing set of 10 Standard Configurations. From the experimental data obtained at the annular test cascade at EPF-Lausanne, Switzerland, two test cases were chosen: A subsonic attached flow case and a transonic separated flow case, which are shown to be suitable for code validations. Hereby experimental effects as well as influences from evaluations have to be taken into account:

The experimental data for the subsonic case is not as sensitive to small flow variations as the off-design transonic case data. Still there are effects in the measured subsonic flow which are not covered by one of the presented 2D/Q3D methods. But all used methods are able to predict the steady flow in a correct range and give the right tendencies of unsteady behavior. For the subsonic case the nonviscous linearized methods are sufficient and most efficient.

The off-design data is much more sensitive to small flow changes. The comparison of calculation results with these data must always take into account the influence of the detailed flow conditions on the pre-shock conditions and the shock position. The separation has a significant influence on the unsteady behavior and in order to correctly predict stability the use of a viscous code is necessary.

The here presented nonlinear Euler model must be improved. The predictions especially for the transonic case could be improved with a better mesh, but still, looking at computing times, the results are not efficient. This is subject of future work.

It is recommended not to use integrated data like the global aerodynamic damping for code validations on such test cases, because the limited number of blade surface measurement points cannot ensure a correct evaluation.

It can be concluded that the quality of the predictions has to be improved, especially for viscous investigations. Furthermore the viscous codes must become cheaper to make them usable. That points out the need of viscous code development and the publication of well documented viscous test data. The published data on STCF 11 contributes to that.

ACKNOWLEDGEMENTS

The measurements were taken during a joint project with Rolls Royce plc., United Kingdom, ABB Power Generation Ltd., Switzerland, Volvo Aero Corporation, Sweden, the Swiss Federal Institute of Technology, Switzerland and the Royal Institute of Technology, Sweden. The authors wish to thank all partners for their collaboration. Special thanks are directed to ABB Power Generation Ltd. for the permission to publish the experimental data, to Rolls Royce for the provision of FINSUP, GE Aircraft Engines for the provision of NOVAK and Volvo Aero Corporation for the provision of VOLFAP, to Mr. L. Imfeld and Mr. T. Börjesson for their contribution to the numerical calculations and for fruitful discussions and to Mr. W. Höhn for the contribution to the mesh generation for INST.

REFERENCES

Anderson, W.K.; Thomas, J.L.; van Leer, B.; 1987
"A Comparison of Finite Volume Flow with Shock Waves"; AIAA Paper 87-1152

Baldwin, B. and Lomax, L.; 1978
"Thin Layer Approximation and Algebraic Model for Separated Turbulent Flow"; AIAA Paper 78-257; 197883

Beam, R.M. and Warming, R.F.; 1977
"An Implicit Factored Scheme for the Compressible Navier Stokes Equations"; Proceedings of the 3rd Computational Fluid Dynamics Conference, Albuquerque, New Mexico

Bölcs, A., Körbächer,H.; 1993
"Periodicity and Repetivity of Unsteady Measurements of an Annular Turbine Cascade at Off-Design Flow Conditions"; ASME Paper 93-GT-107

Bölcs, A., Fransson, T.H., Körbächer,H.; 1991
"Time-Dependent Pressure Fluctuations on an Oscillating Turbine Cascade at Transonic Off-Design Flow Conditions'' in: Unsteady Aerodynamics, Aeroacoustics and Aeroelasticity of Turbomachines and Propellers, H.M. Atassi (ed.), Springer Verlag, New York, pp. 547-565, 1993

Bölcs, A.; Fransson, T.H.; Platzer, M.F.; 1989
"Numerical Simulation of Inviscid Transonic Flow Through Nozzels With Fluctuating Back Pressure"; ASME Journal of Turbomachinery, Vol. 111, pp. 169-180, 1989

Bölcs, A., Fransson, T.H.; 1986
"Aeroelasticity in Turbomachines, Comparison of Theoretical and Experimental Cascade Results"; Communication de Laboratoire de Thermique Apliquée et de Turbomachines, No 1, EPF Lausanne, Switzerland, 1986

Bölcs, A.; 1983
"A Test Facility for the Investigation of Steady and Unsteady Transonic Flows in Annular Cascades"; ASME Paper 83-GT-34, 1983
Carstens, V., Bölcs, A, Körbächer,H.; 1993
Comparison of Experimental and Theoretical Results for Unsteady Transonic Cascade Flow at Design and Off-Design Conditions ASME Paper 93-GT-100
Fransson, T.H., Verdon, J.M.; 1991
"Updated Report on Standard Configurations for Unsteady Flow Through Vibrating Axial-Flow Turbomachine Cascades"; Report Royal Institute of Technology , Stockholm, Sweden
avialable on internet via http://www.egi.kth.se/ekv/stcf
Fransson, T.H., Verdon, J.M.; 1991
"Standard Configurations for Unsteady Flow Through Vibrating Axial-Flow Turbomachine Cascades" in: Unsteady Aerodynamics, Aeroacoustics and Aeroelasticity of Turbomachines and Propellers, H.M. Atassi (ed.), Springer Verlag, New York, pp. 859-889, 1993
Fransson, T.H., Pandolfi, M.; 1986
"Numerical Investigation of Unsteady Subsonic Compressible Flows Through an Oscillating Cascade"; ASME Paper 86–GT-304
Gerolymos, G.A., Vallet, I.,; 1994
"Validation of 3D Euler Methods for Vibrating Cascade Aerodynamics"; ASME Paper 94-GT-294
Giles, M. B.; 1989
"Non-Reflecting Boundary Conditions For Euler Equation Calculations", AIAA Journal, Vol. 28, No. 12, pp 2050-2058
Giles M., Heimes, R.; 1993
"Validation of a Numerical Method for Unsteady Flow Calculations"; ASME, Vol. 115, pp. 110-117
Grüber, B., Carstens, V.; 1996
"Computation of the Unsteady Transonic Flow in Harmonically Oscillating Turbine Cascades Taking Into Account Viscous Effects"; ASME Paper 96-GT-338
Groth, J.P., Mårtensson,H., Eriksson, L.E.; 1996
"Validation of a 4D Finite Volume Method for Blade Flutter"; Turbo Expo, Birmingham, 1996
Hall, K.C., Crawley, E.F.; 1989
"Calculation of Unsteady Flows in Turbomaschinery Using the Linearized Euler Equations"; AIAA, Vol. 27, pp 778-787
He, L.; 1989,
"An Euler Solution for Unsteady Flow Arround Oscillating Blades"; ASME paper 89-GT-279
Holmes, D.G., Chuang, H.A.; 1991
"2D Linearized Harmonic Euler Flow Analysis for Flutter and Forced Response" in: Unsteady Aerodynamics, Aeroacoustics and Aeroelasticity of Turbomachines and Propellers, H.M. Atassi (ed.), Springer Verlag, New York, pp. 213-230, 1993
Huff, D.L.; 1991
"Unsteady Flow Field Predictions for Oscillating Cascades" in: Unsteady Aerodynamics, Aeroacoustics and Aeroelasticity of Turbomachines and Propellers, H.M. Atassi (ed.), Springer Verlag, New York, pp. 127-148, 1993
Imfeld, L.; 1997
"Numerical Determination of Unsteady Flow Through Vibrating Turbomachine-Cascades: International Standard Configurations 4 and 11 with the NOVAC2D60 Code"
Diploma Thesis, KTH Stockholm, 1997
Jöcker, M.; 1994
"Validation of Unsteady Aerodynamic Prediction Models on the Turbine Configuration TCT III" Project Study, KTH Stockholm, 1994
Kahl, G., Klose, A.; 1991
"Time Linearized Euler Calculations for Unsteady Quasi-3D Cascade Flows" in: Unsteady Aerodynamics, Aeroacoustics and Aeroelasticity of Turbomachines and Propellers, H.M. Atassi (ed.), Springer Verlag, New York, pp.109–126, 1993
Krainer, A., Hambraeus, T., Fransson, T.H.; 1997
"Highly Nonreflecting Boundary Conditions for Nonlinear Euler Calculations of Unsteady Turbomachinery Flows"; Proposed Paper submitted to AIAA Journal of Propulsion and Power
Leyland, P., Ott. P., Richter, R.; 1994
"Turbine Cascade Calculations With Structured and Unstructured Meshes"; presented at "Second Computational Fluid Dynamics Conference", ECCOMAS, Stuttgart 1994
Norryd, M., Bölcs, A.; 1997
"Experimental Investigation Regarding Evolution of Unsteady Pressure in a Vibrating Turbine Cascade With Tip Gap Effects"; presented at the 8th International Symposium on Unsteady Aerodynamics and Aeroelasticity of Turbomachines, Stockholm 1997
Ott, P., Norryd, M., Bölcs, A.; 1998
"The Influence of Tailbords on Unsteady Measurements in a Linear Cascade"; Submitted to ASME to be presented in Stockholm 1998
Ott, A.; Bölcs, A.; Fransson, T.H.; 1995
"Experimental and Numerical Study of the Time-Dependent Pressure Response of a Shock Wave Oscillating in a Nozzle" Journal of Turbomachinery, January 1995, Vol. 117, p. 106–114
Rolls Royce; 1989
"FINSUP User Guide and Reference Manual, Issue 2"; Rolls Royce Commercial Technology; Rolls Royce plc. , England
Sidén, G.; 1991
"Numerical Solution of Viscous Compressible Flows Applied to Turbomachinery Blade Flutter"; Ph. D. Thesis, Chalmers University of Technology, Göteborg 1991
Smith, T.E.; 1989
"A Modal Aeroelastic Analysis Scheme for Turbomachinery Blading"; NASA Report CR-187089
Smith, S.N.; 1972
"Discrete Frequency Sound Generation in Axial Flow Turbomachines"; Reports and Memoranda No. 3709, Cambridge 1972
Verdon, J.M., Caspar, J.K.; 1984
"A Linear Aerodynamic Analysis For Unsteady Transonic Cascades"; NASA-CR, 3833
Whitehead, D.S.; 1990
"A Finite Element Solution of Unsteady Two-Dimensional Flow in Cascades"; International Journal of Numerical Methods in Fluids, Vol. 10
Whitehead, D.S., Newton, S.G.; 1985
"A Finite Element Solution of Unsteady Two-Dimensional Transonic Flows in Cascades"; International Journal of Numerical Methods in Fluids, Vol. 5, pp. 115-132, 1985

ATTACHMENT: Table of Test Cases on STCF 11

Steady Data

case	M_1	β_1	M_{2is}	β_2	p_{t1}	p_1	p_2
	-	deg.	-	deg.	mbar	mbar	mbar
100	0.31	15.2	0.69	-66.7	1246	1164	907
200	0.4	34.0	0.99	-	2298	2063	1224

Unsteady Data

case	flow	IBPA (deg)	f (HZ)	k
101	subsonic	18	209	0.2134
102	subsonic	36	209	0.2134
103	subsonic	54	209	0.2134
104	subsonic	72	209	0.2134
105	subsonic	90	209	0.2134
106	subsonic	108	209	0.2134
107	subsonic	126	209	0.2134
108	subsonic	144	209	0.2134
109	subsonic	162	209	0.2134
110	subsonic	180	209	0.2134
111	subsonic	198	209	0.2134
112	subsonic	216	209	0.2134
113	subsonic	234	209	0.2134
114	subsonic	252	209	0.2134
115	subsonic	270	209	0.2134
116	subsonic	288	209	0.2134
117	subsonic	306	209	0.2134
118	subsonic	324	209	0.2134
119	subsonic	342	209	0.2134
201	transonic off-design	36	211.9	0.1547
202	transonic off-design	72	212.1	0.1549
203	transonic off-design	108	212.1	0.1549
204	transonic off-design	144	211.9	0.1547
205	transonic off-design	180	211.6	0.1545
206	transonic off-design	216	212.1	0.1549
207	transonic off-design	252	212.1	0.1549
208	transonic off-design	288	212.1	0.1549
209	transonic off-design	324	212.1	0.1549
210	transonic off-design	360	212.1	0.1549